Studies of Solution Character by Molecular Spectroscopy. 7. Ion Sites for $NaCo(CO)_4$ in Oxetane, 1,2-Dimethoxyethane, and Tetrahydrofuran from 300 to 150 K[1]

Walter F. Edgell,* Shankar Hegde, and Angelo Barbetta

Contribution from the Department of Chemistry, Purdue University, West Lafayette, Indiana 47907. *Received October 6, 1976*

Abstract: Improvements have been made in the techniques for obtaining and analyzing the spectral contours of infrared bands from dissolved salts. The infrared spectra of $NaCo(CO)_4$ solutions with oxetane, 1,2-dimethoxyethane, and tetrahydrofuran as the solvent were obtained over a wide temperature range. These spectra are complex. The presence of three kinds of ion sites is found in these solutions using a computer-aided method of analysis. The spectrum of the $Co(CO)_4^-$ ion in each of the three kinds of ion sites is extracted from the complex spectra. Each such spectrum may be used to identify the site in other solutions. The three kinds of ion sites found are a solvent-separated ion pair site of T_d structural symmetry (type I), a contact ion pair site of C_{3v} structural symmetry (type II), and a triple ion site also of C_{3v} symmetry in the solution structure at the $Co(CO)_4^-$ ion (type III). Only the type I site occurs in the oxetane solution; type I and type II sites are found in the dimethoxyethane solutions; and all three sites are found in the tetrahydrofuran solutions. Type II and type III sites are converted to type I sites as the temperature drops; the intensity of the infrared bands from the type II sites fades faster than those from type III site in tetrahydrofuran solutions. The vibrational spectra at the ion sites follow dual symmetry selection rules. Some consideration is given to a quantum description of the states of these solutions. These ideas are applied to a discussion of the transitions which generate the observed bands and what properties they probe. They are used also to show that one can give meaning to the words structure and symmetry in the solution environment where the conformation is continuously changing. An explanation for the differences in the ion site structure of these three solutions is given in terms of the known properties of the three solvents and the postulate that the interaction of the Na^+ ion with a negative center of a neighbor species is the primary interaction which lowers the free energy of the solution.

Structure in electrolytic solutions is of interest in a number of areas of chemistry. It can contribute to an understanding of the mechanism of chemical reactions in such solutions and to how catalysts for them operate. It can serve as a starting point for the interpretation of macroscopic physical properties of ionic solutions in microscopic terms.

In previous work from this laboratory, the contour of the infrared bands arising from the CO stretching vibrations of the $Co(CO)_4^-$ ion was found to yield a sensitive indication of the ion site structure of nonaqueous solutions.[2] Thus, it was possible to detect two kinds of ion sites for $NaCo(CO)_4$ in tetrahydrofuran.[2,3] These results launched an extensive study in this laboratory of ion sites in a variety of solvents. The objectives of this study are to determine how many different kinds of sites exist in each solution, to identify them, and to learn something about the role of the solvent and its nature in establishing which ion site or mix of ion sites exist in a given solution. The experimental and analytical methods developed for the study have been reported and applied to $NaCo(CO)_4$ solutions with six different solvents, each of which yields a solution with simple site structure.[4] The power of the methods was demonstrated by the fact that they were able to detect the ion site with an isotopic ^{13}C atom even though a clearly separate isotopic band is not seen.

In this paper, further improvements are reported in both experimental and analytical procedures. They are applied to a study of the structure in $NaCo(CO)_4$ solutions with oxetane, 1,2-dimethoxyethane (DME), and tetrahydrofuran (THF) as solvents. These studies were made at 300 K and at lower temperatures in 25 °C intervals throughout the liquid state range. The lowest temperature studied was 200 K in oxetane and DME solutions and 150 K in THF solutions. An explanation is offered for the different structure observed in each of these solutions. And some consideration is given to the quantum states of solutions and to their excitation to produce the infrared bands of this study.

Experimental Section

Chemicals. The oxetane and DME used in this study were obtained from Pfaltz and Bauer, Inc., and the THF from the Fisher Scientific Co. The $Co_2(CO)_8$ and CaH_2 were from Alpha Inorganics, the Na/K alloy (78% K; 99.95% pure) from M.S.A. Research Corp., and the molecular sieves (4 Å, pellets) from Union Carbide—Linde Division. The NaOH was a Mallinckrodt analytical reagent.

$NaCo(CO)_4$ Preparation. The salt $NaCo(CO)_4$ was prepared by the reaction of $Co_2(CO)_8$ with NaOH in THF,[5] using the procedure outlined in ref 4. The freedom of the salt from H_2O and THF was established as indicated earlier.[4]

Solvent Preparation. DME and THF were dried in two stages. In the first stage, these solvents were deaerated and dried with molecular sieves as indicated earlier.[4] Then 100 g of the sieve-dried solvent was shaken with 1 g of Na/K alloy for 6 h and filtered through a fine glass frit. Oxetane polymerizes on contact with molecular sieves and reacts with Na/K alloy. It was deaerated and vacuum distilled into an empty flask and then treated for 24 h with CaH_2, followed by filtration. The residual water in these solvents was less than that which could be detected by the spectroscopic method,[4,6] i.e., $\leq 3 \times 10^{-5}$ mol H_2O/L solvent.

Solution Preparation. The $NaCo(CO)_4$ solutions were prepared as indicated earlier in order to prevent their contamination with H_2O or reaction with O_2.[4] The concentration of each solution was determined by weighing the salt into a volumetric flask and adding solvent to the mark. The concentration used in each case was near 1.2×10^{-3} M.

Low-Temperature Production. The source of the cooling used to produce the low temperatures of this study was an Air Products and Chemicals AC-3L Cryotip cooler which operates on the open-cycle, Joule-Thomson principle.[7] While this unit was designed to operate with compressed He and H_2, we had no need for such low temperatures in this work. Therefore, compressed N_2 was used in the He circuit—a mode of operation which could reach 80 K. The temperature reached at the cryotip was controlled by the pressure of N_2 at the entrance of the Joule-Thomson expansion circuit. A two-stage regulator was used to control this pressure.

The infrared cell was screwed into the cryotip by means of its threaded shaft (see below). A ring of indium metal was placed between

0002-7863/78/1500-1406$01.00/0

the top of the mounting screw and the cryotip and was squeezed flat as the cell was screwed into the cryotip. This provided good thermal contact between the cell and the cold tip. In order to reduce the thermal flow from the room to the infrared cell, the cell and cryotip were mounted in a stainless steel, vacuum-tight shroud, with polytran KCl windows for the passage of the infrared beam. The pressure in the region surrounding the cell and cryotip was kept at $\leq 10^{-5}$ mmHg with a mercury diffusion pump (Edwards Model EM2) backed by a Edwards ES35 forepump. An all-metal vacuum system was used.

The temperature was measured with a chromel vs. constantan thermocouple sealed to the end of the cryotip. The reliability of the temperature measured in this way was determined in the following manner. The cell was filled with pure, dry THF and the above system placed into operation. Cooling was continued until the THF froze. Cooling was then discontinued and the system slowly warmed up, the temperature being monitored with the thermocouple. In repetitive trials, the THF melted with a sharp melting point, which, when measured by the thermocouple, was always within 1 °C of the accurate melting point of the sample measured separately. During the course of an infrared run, the temperature was held within 1 °C of the stated value as measured by the thermocouple.

Infrared Cell. An exploded view of the low-temperature cell is shown in Figure 1. The cell holder consists of a base plate and a top ring and was made of copper in the department shop. The wave washers were also made there. The gaskets and the cell spacer were made of indium foil obtained from the Indium Corporation of America. The polytran CaF_2 windows (32 × 3 mm disks) were obtained from the Harshaw Chemical Co., the Monel needle plate from the Barnes Engineering Co., and the molded Nylon screws ($\frac{1}{8}$ in.) from the Weckesser Co. The Luer-Lok syringe tips, which are part of the needle plate as received, were removed and the filling ports threaded.

The liquid cell is formed by an indium spacer pressed between the two CaF_2 windows. The windows must withstand the stresses in the cell as the temperature is changed and should not be attacked by moisture in the air or the solvents of this study. Amorphous CaF_2 windows serve these purposes well. The cell must remain vacuum tight (external pressure $\leq 10^{-5}$ mmHg) over a temperature range of 300–80 K. It is sealed by pressure applied through the six screws distributed around the perimeter of the cell holder, which are tightened until the indium beings to flow. The indium gaskets introduced between (1) the base and the back window and (2) the front window and the needle plate avoid the cracking of the windows when the pressure is applied. The compression of the wave washer serves to keep all parts of the cell in close contact when the temperature changes. Access to the sample volume is provided by the two filling ports in the needle plate through the two holes drilled in the front CaF_2 window. A vacuum-tight seal of the access ports is made by placing small indium pieces in each port and then closing them with metal screws which forces the indium metal into all interstices. The cell is opened by removing the screws and scratching the indium plugs with a needle.

The cell is easy to assemble and disassemble for cleaning and is transparent in the region from 0.125 to 12 μm. It operates reliably and has been repeatedly cycled between 300 and 100 K under vacuum ($\leq 10^{-5}$ mmHg) without leaking. However, the windows are not sufficiently parallel to give interference fringes with infrared radiation.

Infrared Spectra. All the spectra were recorded between 1800 and 2030 cm^{-1} with a Perkin-Elmer 180 spectrophotometer using the linear absorbance scale. The spectra were obtained with an expanded abscissa scale of 1 cm^{-1}/2 mm in order to reveal all details of the band contour. The instrument was operated in the constant I_0 energy mode at a scan rate of 12 cm^{-1}/min. The slit width varied from 0.20 to 0.23 mm over a run, which corresponds to a resolution change from 1.0 to 1.4 cm^{-1}. Under these conditions, there is no tracking error or band distortion for the bands under study.[8] The wavenumber correction was made as reported elsewhere.[4] Each spectrum was traced twice on the same chart paper. The two tracings superimposed on each other within the noise level in the spectra.

It is necessary to separate the absorption due to the salt from that of the solvent. This was accomplished in two stages. The low-temperature cell was filled with solvent and placed in the cooling apparatus in the sample beam of the spectrometer. A variable path cell was filled with solvent and placed in the reference beam. Its path length was adjusted until there was the same amount of solvent in each beam as evidenced by the fact that the spectrometer tracing was a straight line. Then the desired temperature of the sample cell with solvent was established and a spectral tracing made. Only one cooling system is available so the reference cell with solvent remains at room temperature. Since the solvent spectrum varies with temperature, the spectral tracing deviates from a straight line when the sample cell with solvent is not at ambient temperature. A "solvent" spectral tracing is made for each temperature to be studied in the run. Then the cooling system is allowed to return to room temperature, and the sample cell removed, emptied of solvent, and filled with solution, using the techniques described elsewhere.[4] The sample cell with solution was placed again in the cooling system and the solution tracing recorded at each temperature. The two tracings at each temperature, solution and "solvent", permit the solvent contribution to the solution spectrum to be removed.

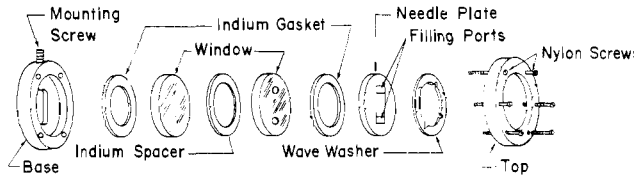

Figure 1. Exploded view of the low-temperature cell.

Results

THF melts at 165 K.[9] It was found possible to supercool the $NaCo(CO)_4$ solutions in this solvent as well as the pure solvent. Spectral tracings for the liquid state were made at 300, 275, 250, 225, 200, 175, and 150 K. It was found that the solution spectrum falls to the solvent spectrum in both wings of the band contour. This is a characteristic of each run made in this study. It means that, with the dilute solutions used here, it is possible to reliably remove the contribution of the solvent from the solution spectrum by subtracting the absorbance of the solvent from that of the solution. This reduces, in the experimental procedure used here, to substracting the absorbance of the "solvent" tracing from that of the solution tracing. The spectrum of the dissolved salt, arrived at in this way, is shown in Figure 2 for the seven temperatures of this study.

1,2-DME freezes at 215 K.[9] It was also possible to supercool this solvent and its $NaCo(CO)_4$ solution. Spectral tracings were made of the liquid state samples at 300, 275, 250, 225, 215, and 200 K. The absorbance due to the solvent was subtracted from the solution spectra to give the spectra of the dissolved salt shown in Figure 3.

Oxetane freezes at 171 K as measured with a differential scanning calorimeter. Spectral tracings were made at 300, 275, 250, 225, and 200 K. The spectrum of the dissolved salt at these temperatures is shown in Figure 4.

These spectra arise from the C–O stretching vibrations of the $Co(CO)_4^-$ ion.[10] They can be expected to be complex when the anion exists in more than one ion site in the solution.[2,3] The spectrum of $NaCo(CO)_4$ in THF is in qualitative agreement with that reported earlier.[3] The presence of three component bands in the complex spectrum is readily seen. The bands at 1855 and 1899 cm^{-1} lose intensity as the solution temperature falls while that at 1886 cm^{-1} gains intensity. These intensity variations result from changes in the population of the ion sites. In contrast, the spectrum of the salt in oxetane consists of a single strong band whose peak intensity and bandwidth are given in Table I. The very weak side band at 1853 cm^{-1} in the oxetane solution spectra and in the THF solution spectrum at 150 K arises from the mono-C(13)O species due to the natural abundance (1.1%) of ^{13}C in the sample.[4] The band contour for $NaCo(CO)_4$ in 1,2-DME at first glance appears to be similar to that from the oxetane solution. Careful scrutiny of the band envelope for the DME solutions, however, will indicate that the situation is more complicated than appears from a visual examination; and we shall see that such complexity also exists in the contour from the THF solution.

To proceed further it is necessary to analyze the spectra

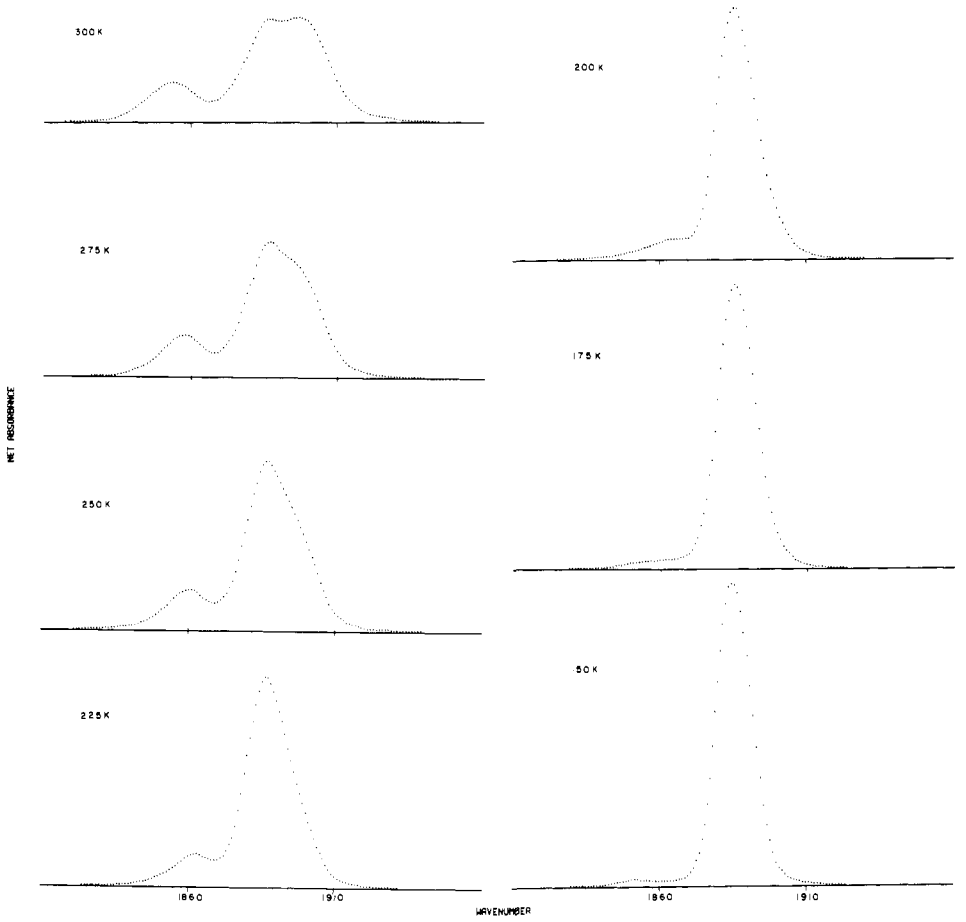

Figure 2. The infrared spectrum of $NaCo(CO)_4$ when dissolved in THF, 150–300 K.

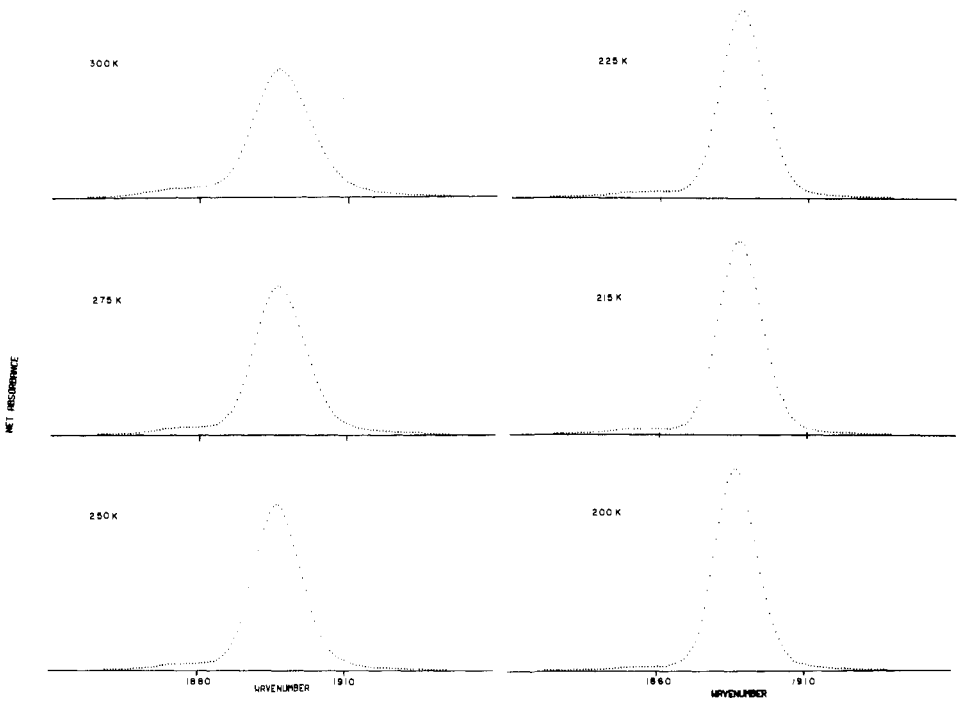

Figure 3. The infrared spectrum of $NaCo(CO)_4$ when dissolved in 1,2-DME, 200–300 K.

quantitatively to find the component bands which overlap each other to produce the complex spectral contour. The single CO stretching band of $Co(CO)_4^-$ arising from the single ion site found in the previously studied solutions has neither the Gauss nor the Lorentz contour.[4] It was represented analytically in the previous study from this laboratory by a sum of a Gauss and a Lorentz contribution,[4] or more precisely by

$$A(\omega) = \alpha + G(\omega) + L(\omega) \quad (1)$$

where $A(\omega)$ is the absorbance at the wavenumber ω and $G(\omega)$

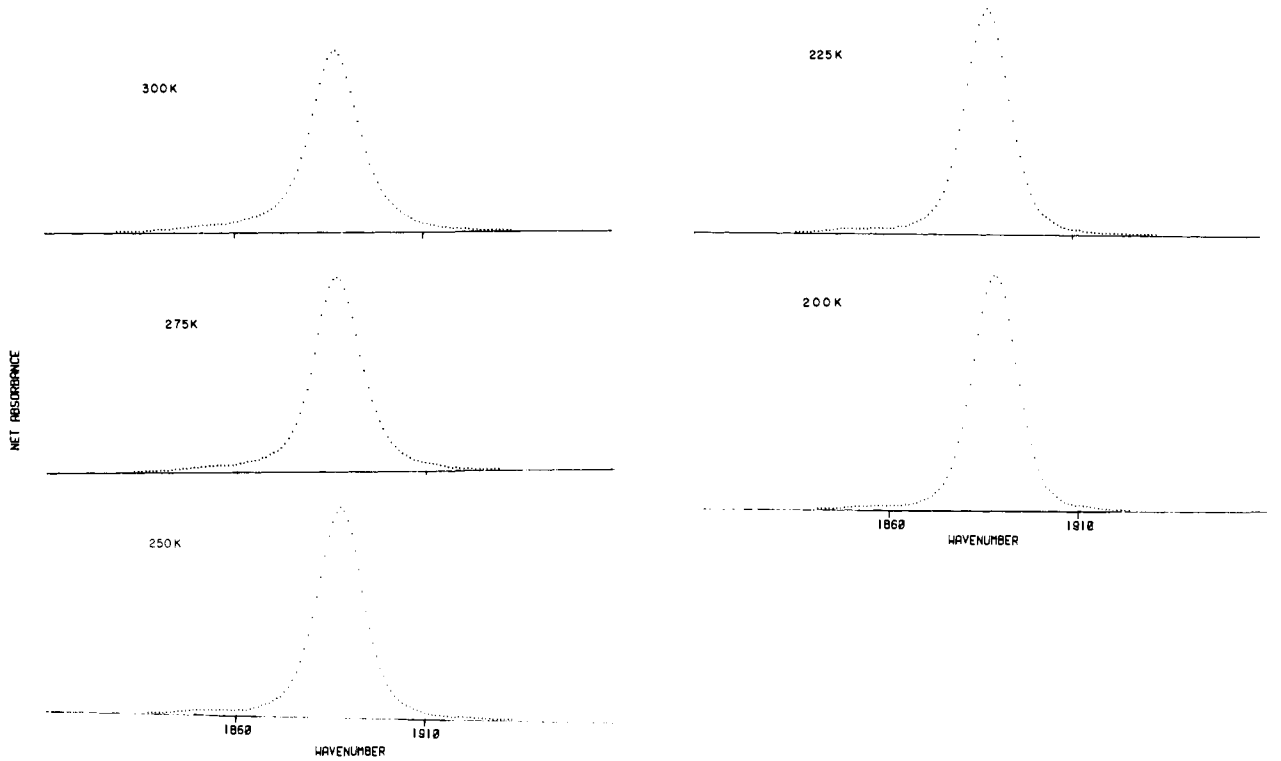

Figure 4. The infrared spectrum of $NaCo(CO)_4$ when dissolved in oxetane, 200–300 K.

and $L(\omega)$ are the Gauss and Lorentz contributions. Here α is a small contribution added to correct the baseline. The parameters which define $G(\omega)$ and $L(\omega)$ (plus α) are selected by a nonlinear, least-squares procedure which maximizes the fit of the analytical expression to the experimental band. To represent the dominant band from the oxetane solutions, it is necessary to use a small negative value of α. It is very common for α to have a positive value.[11,12] Such a value may be explained by background absorption which might result from (1) extensions of the wing elements of remote bands and (2) imperfect cell matching with incomplete solvent compensation.[12] In all spectra we have recorded here the solution spectrum *coincides* with the solvent spectrum in both wings of the overlapped system and hence there is no justification for the use of a nonzero value of α, either positive or negative. When α is set to zero, it is not possible to represent the data from the oxetane solution satisfactorily with eq 1.

One consequence of not including all the absorbance associated with each component band of an overlapped system in the mathematical representation is that one assigns the "extra" absorbance to the presence of one or more spurious bands. Assigning too much absorbance to each component band leads to equally erroneous results. Therefore, we sought to find a better representation of a single component band than eq 1, using the oxetane data as the test case. It was found that the sum of two different Lorentz contributions or two different Gauss contributions were no improvement over eq 1. Surprisingly, the sum of one Gauss and two different Lorentz contributions did little better, even though there were more parameters which were adjusted to get the best fit. Any of these sums could be made to fit the experimental contour well in the central region of the band but not simultaneously in its wings. This might explain the role played by the nonzero value of α in eq 1.

It was possible, however, to fit the band very well in both the central region and the wings by the sum of three different Gauss contributions, i.e., by eq 2,

$$A(\omega) = h_1 \exp(-d_1^2(\omega - \omega_0)^2) + h_2 \exp(-d_2^2(\omega - \omega_0)^2) + h_3 \exp(-d_3^2(\omega - \omega_0)^2) \quad (2)$$

Table I. Peak Absorbances and Bandwidths for $NaCo(CO)_4$ in Oxetane Solution at Various Temperatures

Temp, K	Peak absorbance	Half-width, cm^{-1}
300	0.508	15.5
275	0.542	14.5
250	0.587	14.0
225	0.629	13.8
200	0.654	13.6

with ω_0 being the wavenumber of the band center and h_1 the peak absorbance of the first Gauss contribution while d_1 describes its half-width through the relation

$$d_1 = \sqrt{\ln 2}/\mathrm{GHW}_1$$

Here GHW_1 is half the width of the first Gauss contribution at half its peak absorbance. The parameters h_2 and d_2 similarly describe the second Gauss contribution to the band (also centered at ω_0) while h_3 and d_3 do the same for the third contribution. The absorbance A of a complex spectrum consisting of several overlapped bands is given by

$$A(\omega) = \sum_i A_i(\omega) \quad (3)$$

where the absorbance of the ith component band, $A_i(\omega)$, is given by eq 2 and the sum is over all the bands whose overlapping make the complex spectral contour.

The spectrum from the oxetane solution at room temperature consists of a single band only slightly overlapped in one wing by the very weak band from the isotopic ions. Therefore, it furnishes a good test of the ability of eq 2 to represent the contour of a single band. How well eq 2 can do this is seen in the comparison of the experimental contour for the oxetane band with the calculated contour shown in the upper left hand frame of Figure 5. The calculated contours of the two component bands of this spectrum, one from the normal ions and one from the isotopic ions, are shown in the second frame on the left of Figure 5. Their sum, of course, is the calculated contour shown in the first frame. The seven parameters used

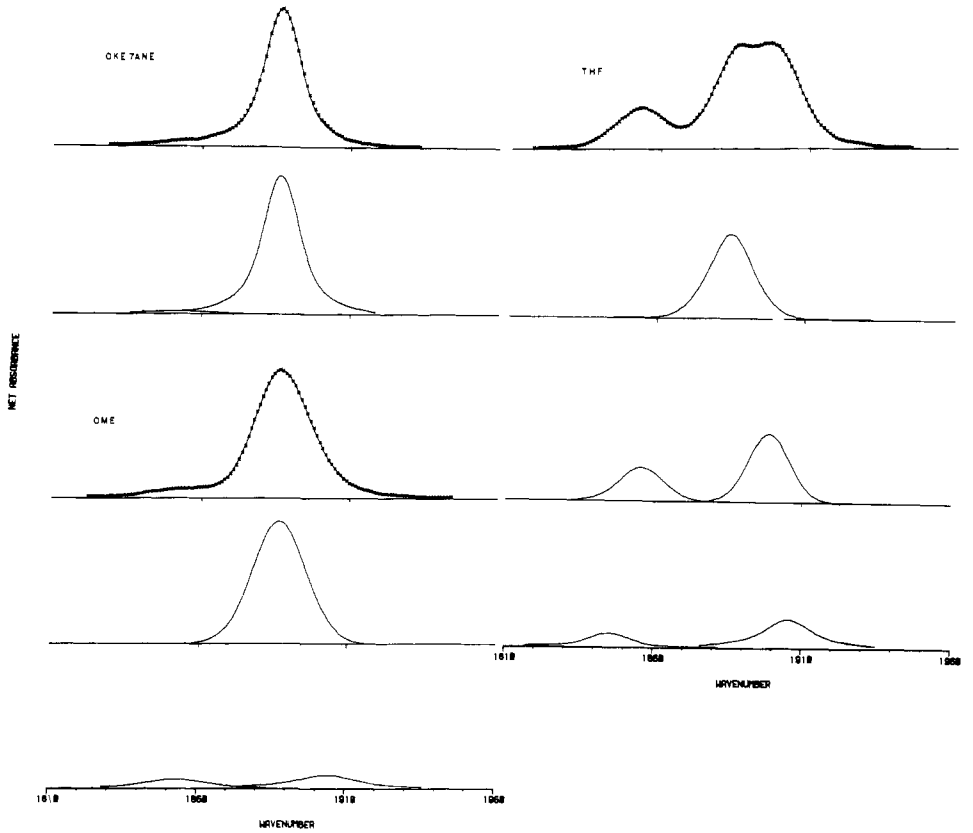

Figure 5. The comparisons of the experimental and computed spectra at 300 K. The component bands of the computed spectra. Left column: Frame 1, xxxx experimental spectrum, salt in oxetane, — computed spectrum; frame 2, the two component bands of the computed spectrum; frame 3, xxxx experimental spectrum, salt in 1,2-DME, — computed spectrum; frame 4, the computed band type I site; frame 5, the computed bands type II site. Right column: frame 1, xxxx experimental spectrum, salt in THF, — computed spectrum; frame 2, the computed band type I site; frame 3, the computed bands type II site; frame 4, the computed bands type III site.

to describe the band for the normal ion (ω_0, h_1, d_1, h_2, d_2, h_3, and d_3) are collected in the first line of Table II.

A comment on how these values are obtained is in order. These seven parameters plus the seven used to describe the isotopic band were fixed by a nonlinear, iterative procedure which maximizes the fit of the computed contour to the experimental contour by minimizing the sum over each measured point of the spectrum of the square of the weighted difference between the experimental and the calculated absorbance there. The computer program used to carry out this iterative procedure is similar to one described recently[13] but uses eq 2 to calculate $A_i(\omega)$. Its spirit is taken from the work of Pitha and Jones.[14]

Application of this technique of contour representation to the spectra of $NaCo(CO)_4$ in oxetane at 275, 250, 225, and 200 K shows that each spectrum consists of (1) a strong, main band centered at 1887 cm^{-7} and (2) a very weak side band centered at 1853 cm^{-1}. The comparison of the experimental spectrum with the spectral contour calculated on this basis from the best band parameters for each of the two bands is shown for each of these temperatures in Figure 6. The computed contours are seen to be an excellent representation of the experimental spectra and demonstrate that eq 2 is able to represent the changing character of this band as the temperature falls. The seven parameters found to describe each band at each temperature are collected in Table II.

The spectra for $NaCo(CO)_4$ dissolved in 1,2-DME appear to result from two overlapped bands also. However, the best spectral contour calculated on this basis does not furnish a satisfactory representation of the experimental spectrum at any temperature. The differences between the experimental and calculated spectra indicate the presence of a second weak, overlapped band on the high-wavenumber side of the main band. Good agreement with the experimental spectra is obtained when the computer is directed to find the best spectral contour composed of three bands. The central parts of each of these three bands for 300 K are shown in frames 4 and 5 on the left of Figure 5. Their sum to give the calculated spectral contour is given in frame 3. It can be seen to be in excellent agreement with the observed spectrum. Figure 7 shows the computed spectral contour and the experimental spectrum at each reduced temperature, as well as the three component bands comprising the computed spectra. The agreement between the two is equally good at these temperatures. The parameters which describe these bands at each temperature are found in Table III.

Table II. Parametric Description of the Band from the Type I Site for $NaCo(CO)_4$ in Oxetane at Various Temperatures

Temp, K	ω_0, cm^{-1}	h_1	d_1	h_2	d_2	h_3	d_3
300	1853.6	0.005	0.066	0.003	0.055	0.003	0.057
	1886.8	0.356	0.134	0.119	0.065	0.032	0.035
275	1854.3	0.006	0.109	0.002	0.055	0.002	0.036
	1887.2	0.377	0.137	0.140	0.069	0.025	0.036
250	1854.1	0.003	0.150	0.003	0.338	0.006	0.100
	1887.1	0.467	0.134	0.105	0.063	0.013	0.027
225	1853.1	0.003	0.150	0.003	0.338	0.008	0.100
	1887.4	0.470	0.138	0.125	0.077	0.032	0.040
200	1853.1	0.003	0.150	0.003	0.338	0.005	0.100
	1887.1	0489	0.135	0.120	0.092	0.048	0.047

The spectrum of $NaCo(CO)_4$ in THF solution at 300 K clearly shows the presence of three component bands. However, the best calculated spectrum, computed on this basis, is a poor representation of the experimental spectrum. Comparison of the two suggests the presence of an additional weak band in each wing. Excellent agreement between the spectral contour

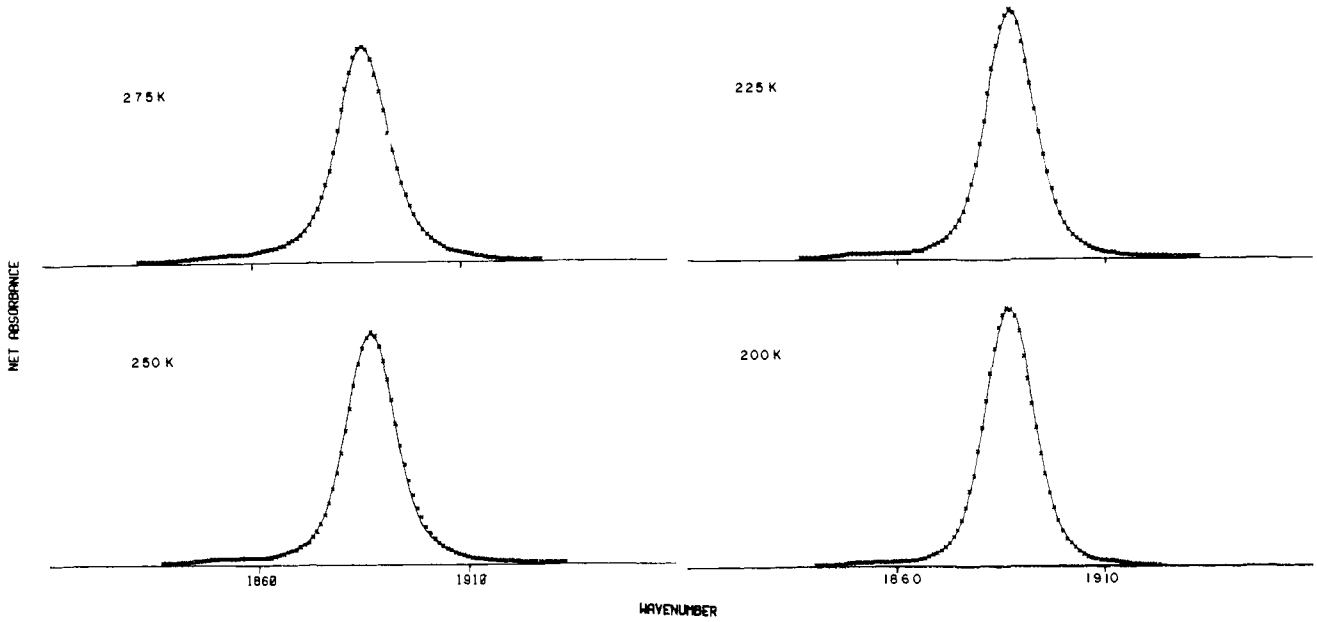

Figure 6. The comparisons of the experimental and computed spectra for $NaCo(CO)_4$ in oxetane at various temperatures. xxxx experimental spectra; — computed spectra.

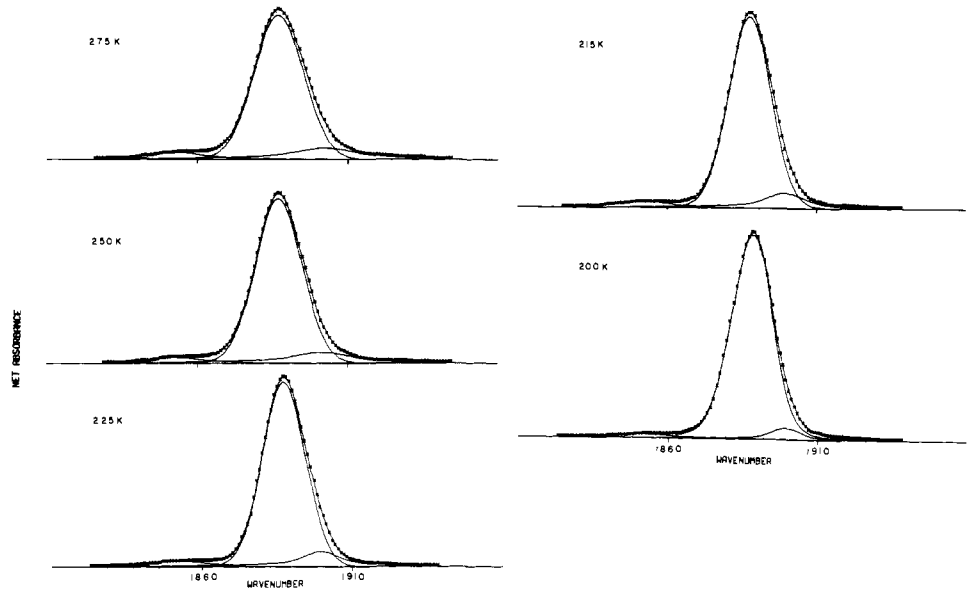

Figure 7. The comparisons of the experimental and computed spectra for $NaCo(CO)_4$ in 1,2-DME at various temperatures. The component bands. xxxx experimental spectra; — computed spectra and also the component bands of the computed spectra.

calculated on the latter basis and the experimental spectrum is readily obtained. It is shown in the first frame on the right of Figure 5. The five component bands whose overlapping give the calculated spectrum are shown in the second, third, and fourth frames on the right of Figure 5. This type of analysis also shows the presence of five component bands in the spectra at 275 and 250 K. These component bands for both temperatures are shown in Figure 8 together with comparisons of the calculated and experimental spectra. In contrast, however, the analysis shows the presence of only three bands at 225, 200, and 175 K. These can be seen in Figure 8 as well as the comparison of the calculated and experimental spectra. The analysis of the spectrum at 150 K shows that the weak absorption on the low-wavenumber side of the main band breaks into two component bands as can also be seen in Figure 8. It is worthy to note that this analysis reproduces each nuance of the experimental spectra over the wide temperature range. The parameters which describe each component band at each temperature are found in Table IV.

Discussion

The previous study[4] of solution structure from this laboratory reported major improvements in the experimental techniques for producing the spectra over those used in the earlier studies[2,3] as well as in the quantitative methods for their analysis. This study presents a further improvement in both the experimental techniques and the methods of analysis. The replacement of the Perkin-Elmer 421 infrared spectrophotometer by the Perkin-Elmer 180 instrument has meant a major improvement in the reproducibility of our spectra. The substantial reduction in the corrections required for the wavenumber scale yields greater wavenumber accuracy. And it is now possible to record the spectra with less noise without sacrificing band contour fidelity. The low-temperature cell is a far cry from that used in the early work. The improvements have come in two stages—the Barbetta thesis and the Hegde thesis. The current cell is leakproof under high vacuum over an extended temperature range, and is reliable and easy to assemble and disassemble. The temperature measurement and

Table III. Parametric Description of the Bands Arising from Each Ion Site for $NaCo(CO)_4$ in 1,2-DME at Various Temperatures

Temp, K	ω_0, cm^{-1}	h_1	d_1	h_2	d_2	h_3	d_3
300	1853.5	0.010	0.034	0.011	0.077	0.013	0.077
	1887.1	0.315	0.074	0.114	0.089	0.019	0.106
	1903.9	0.013	0.025	0.014	0.103	0.022	0.071
275	1853.1	0.006	0.022	0.010	0.073	0.011	0.115
	1887.2	0.384	0.084	0.111	0.093	0.028	0.103
	1902.9	0.014	0.023	0.007	0.119	0.022	0.075
250	1853.5	0.005	0.039	0.011	0.056	0.008	0.186
	1887.3	0.455	0.090	0.109	0.092	0.033	0.146
	1901.9	0.014	0.023	0.007	0.107	0.021	0.089
225	1852.7	0.004	0.136	0.012	0.053	0.006	0.087
	1887.3	0.529	0.097	0.094	0.114	0.044	0.106
	1899.7	0.012	0.023	0.014	0.085	0.030	0.152
215	1852.6	0.007	0.106	0.009	0.053	0.006	0.074
	1887.3	0.557	0.100	0.098	0.117	0.038	0.076
	1899.6	0.012	0.028	0.015	0.091	0.029	0.140
200	1852.4	0.008	0.123	0.002	0.010	0.004	0.044
	1887.5	0.597	0.108	0.102	0.105	0.039	0.046
	1899.7	0.008	0.046	0.009	0.131	0.026	0.170

control have been improved. The solvents are at least five times drier than in the previous study. In fact, it is no longer possible to detect water in them by the spectroscopic method[6]—a method whose lower limit of detectable water has been placed at $\leq 3 \times 10^{-5}$ mol of water per liter of solvent. These improvements have made it possible to extend the work to the tenfold more dilute region of 10^{-3} M—thus approaching closer to the ideal of the salt in an infinitely dilute solution. One benefit of working in such dilute solutions is the ready subtraction of the solvent contribution from the solution spectra. The improvement in the ability to represent the contour of a single band accurately means an improvement in the reliability of the band analysis.

Ion Sites and Their Spectra. Each different kind of ion site for the $Co(CO)_4^-$ ion can be expected to have its own spectrum. The observed spectrum for $NaCo(CO)_4$ in a specific solution (in this region of observation) is just the sum of the spectra from the several kinds of $Co(CO)_4^-$ ion sites present in the particular solution, each weighted by the population of that site. Excluding the isotopic band, only one band, at 1887 cm^{-1}, is seen for the salt in oxetane. Thus, only one kind of ion site is present in this solution. The analysis of the spectra at all temperatures from 300 to 200 K, Figures 5 and 6, shows this same result.

Three bands are found in the spectrum analysis for $NaCo(CO)_4$ in 1,2-DME, Figures 5 and 7. The bands at 1854 and 1899 cm^{-1} fade away together as the temperature of the solution drops. Thus, both bands arise from the $Co(CO)_4^-$ ion in the same site. The population of this site decreases slowly with temperature. In contrast, the intensity of the strong 1887 cm^{-1} increases as the solution temperature drops. Therefore, this band must arise from a second, different kind of site for the $Co(CO)_4^-$ ion. The implication is that the population of this second site increases with decreasing temperature.

The analysis of the spectrum of $NaCo(CO)_4$ in THF at 300 K shows the presence of five bands. These are divided into three groups as shown in frames 2, 3, and 4 on the right of Figure 5 on the basis of the intensity behavior with temperature seen in Figure 8. Only the band at 1885 cm^{-1} increases in intensity with falling temperature. Consequently, it constitutes the spectrum of a $Co(CO)_4^-$ ion site whose population increases

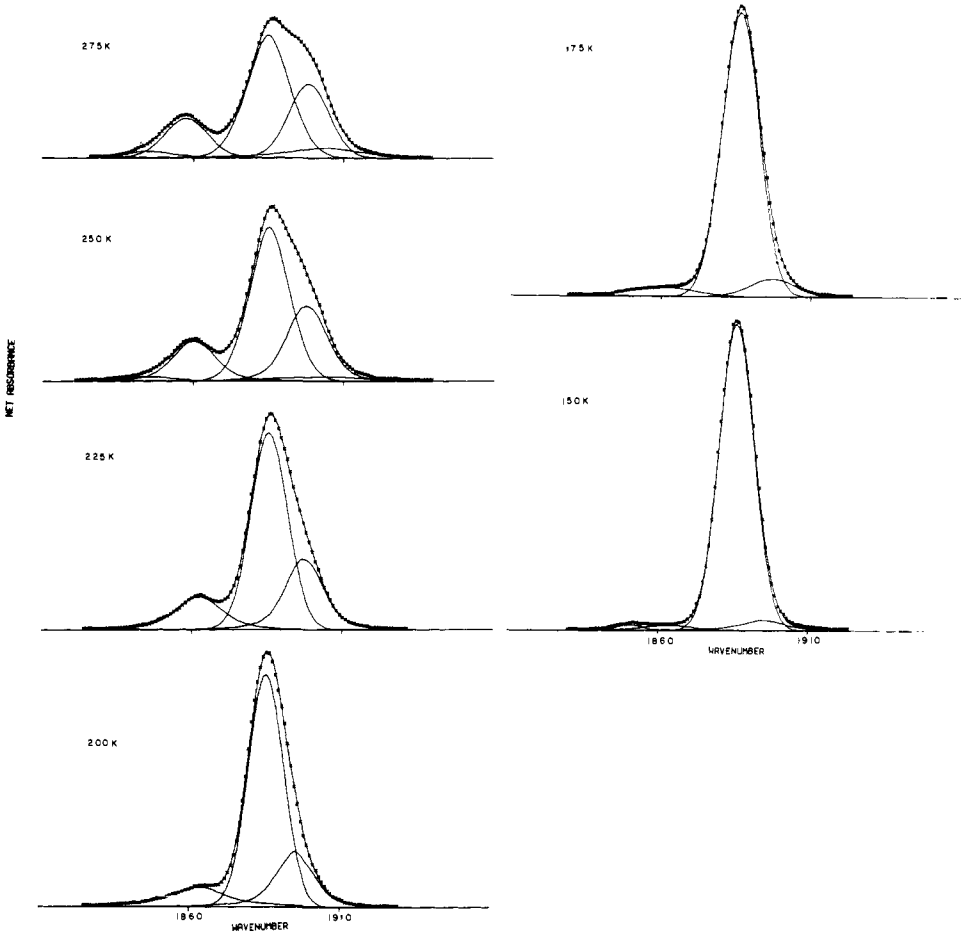

Figure 8. The comparisons of the experimental and computed spectra for $NaCo(CO)_4$ in THF at various temperatures. The component bands of the computed spectra. xxxx experimental spectra; — computed spectra and also the component bands.

Table IV. Parametric Description of the Bands Arising from Each Ion Site for $NaCo(CO)_4$ in THF at Various Temperatures

Temp, K	ω_0, cm^{-1}	h_1	d_1	h_2	d_2	h_3	d_3
300	1845.6	0.009	0.027	0.021	0.111	0.021	0.111
	1855.9	0.064	0.082	0.040	0.112	0.019	0.109
	1884.7	0.248	0.083	0.056	0.164	0.006	0.202
	1898.8	0.191	0.106	0.058	0.092	0.001	0.843
	1905.9	0.018	0.029	0.034	0.059	0.053	0.122
275	1846.0	0.010	0.057	0.007	0.108	0.007	0.109
	1858.1	0.081	0.103	0.047	0.104	0.015	0.072
	1885.4	0.315	0.088	0.093	0.114	0.036	0.247
	1898.8	0.204	0.112	0.064	0.088	0.001	0.583
	1904.0	0.010	0.027	0.022	0.059	0.006	0.180
250	1846.2	0.002	0.064	0.004	0.069	0.010	0.095
	1860.6	0.081	0.096	0.051	0.121	0.012	0.040
	1885.7	0.396	0.098	0.116	0.118	0.045	0.258
	1898.0	0.207	0.119	0.066	0.070	0.001	0.002
	1904.9	0.004	0.032	0.009	0.040	0.003	0.131
225	1862.5	0.067	0.086	0.035	0.136	0.018	0.043
	1886.0	0.489	0.109	0.151	0.132	0.071	0.131
	1897.5	0.192	0.126	0.044	0.079	0.019	0.044
200	1864.0	0.039	0.102	0.027	0.037	0.007	0.158
	1885.9	0.586	0.120	0.173	0.127	0.094	0.124
	1895.4	0.167	0.116	0.014	0.572	0.023	0.041
175	1859.9	0.001	0.133	0.012	0.059	0.023	0.064
	1886.3	0.747	0.112	0.186	0.129	0.096	0.126
	1897.5	0.011	0.073	0.013	0.081	0.042	0.103
150	1851.0	0.004	0.193	0.003	0.157	0.015	0.160
	1864.0	0.002	0.051	0.003	0.050	0.015	0.100
	1886.4	0.858	0.120	0.153	0.136	0.100	0.120
	1895.8	0.009	0.034	0.008	0.170	0.022	0.100

as T goes down. The intensity of each of the other four bands falls with the temperature. The bands at 1846 and 1906 cm^{-1} arise from the anion in a second solution site because they fade away together with dropping temperature and are, in fact, completely missing from the spectrum at 225 K and below; see Figure 8. Since the bands at 1856 and 1899 cm^{-1} also fall off in intensity together, but at a slower rate, they constitute the spectrum of a third site. The population of this site, like that of the second, falls with the temperature.

The spectrum of each of these six sites is shown in a separate frame of Figure 5. One notes that the spectrum of the sole site of the oxetane solution is the same as that of the site whose population dominates the 1,2-DME solution and is also the same as that of a site which comprises some 40% of the ion sites in the THF solution at 300 K. This means that the force field at the $Co(CO)_4^-$ ion is effectively the same in all three sites. It implies that the same kind of solution structure exists at the anion in this site in all three solutions and that the interaction of the solvent molecules with the anion is very similar in these three solvent systems. This site is called a type I site.

Further, the weak spectrum of the other ion site of the 1,2-DME solution is repeated in that of the second site with strong bands from the THF solution. Clearly, these bands arise from the same kind of ion site—an ion site of small population in the 1,2-DME solution but of substantial proportions in the THF solution at 300 K. The fact that the weak bands of the 1,2-DME solutions are repeated with strong intensities in the THF solution, and move together with temperature, is a strong confirmation of their assignment to the same ion site. This site is designated here as a type II site.

The two weak component bands of the anion in THF solution at 300 K comprise the spectrum of a third kind of site—here called a type III site. The fact that they move together with temperature as well as the equally important observation that they are repeated at greater intensity in the site spectra of other solutions (to be reported on later) are strong reasons for assigning both bands to the same site.

Table V. The 2000-cm^{-1} Infrared Bands for the $Co(CO)_4^-$ Ion in the Several Ion Sites Found in Oxetane, 1,2-DME, and THF

Site type	ω, cm^{-1}	Rel intensity	Symmetry	Assignment
I	1887	s	T_d	F_2
II	1899	s	C_{3v}/T_d	E/F_2
	1856	m		A_1/F_2
III	1906	s	C_{3v}'/T_d'	E/F_2
	1846	m		A_1/F_2

The frequency and relative intensities of the infrared bands of these three $Co(CO)_4^-$ ion sites are collected in Table V.

Ion Site Structure and Symmetry. Some comment about the structure and effective vibrational symmetry for the several sites of the $Co(CO)_4^-$ in these three solvents can be made. The species of a solution are in constant turmoil, which produces, in time, a large number of different structural conformations in the environs of a given ion. These conformations in a particular solution may be divided into several groups, the conformations of each group all possessing one or more important structural features in common. These are the different ion sites characterized above by their spectra. To the extent that a classical approximation can be used for a quantum situation, the spectrum for each site is just the sum of that produced on exciting the anion vibrations in each of the conformations of that site, the contribution of each conformation being weighted by its probability of occurrence in the solution. The ions of a given site are expected to produce some order in the arrangement of the solvent molecules in their immediate environs—an order which is greater than that characteristic of the solvent alone but one which rapidly falls to that level as one moves away from the ions. In this sense, one can speak of the ions and the ordered solvent molecules about them on each ion site as forming a solution "structurite".[15] Relaxation studies to be described at another time support this idea.

The $Co(CO)_4^-$ ion has the geometry of a tetrahedron.[10,16] Thus, the spectrum of an isolated $Co(CO)_4^-$ ion would be expected to obey the selection rules for the T_d point group. Of the four C–O stretching modes of vibrations of such an entity, three are degenerates to give the F_2 band in the infrared spectrum while the fourth mode, of A_1 symmetry, is forbidden. If the forces resisting the distortion of the CO bonds of the anion in a given structurite are effectively tetrahedral, its spectrum will follow T_d rules. This is what one observes in the spectra of the type I site. The only probable structural arrangement which can be expected to produce an effective tetrahedral field has solvent molecules as near neighbors of the CO groups of the anion. Then, the Na^+ also has only solvent molecules as near neighbors. Since the dielectric constants of oxetane, 1,2-DME, and THF are all low (ca. 7), most of these ions of the type I site are expected to be associated as solvent-separated ion pairs. Type I structurite, in such a case, can be represented schematically as

```
      S    S  S
S   Na+   S  A-   S
      S    S  S
```

type I structurite

Here S stands for a solvent molecule and A^- for the $Co(CO)_4^-$ anion. The solvent-surrounded, free ions are also expected to give the same spectrum as that of the above structurite. Both of these cases are referred to as type I ion sites.

When the near neighbors of the $Co(CO)_4^-$ ion make one CO moiety substantially different from the other three, the threefold degeneracy of the F_2 modes is partially lifted. This kind of structure occurs when the anion replaces a solvent

molecule in the near neighbor shell of the Na^+ ion. This forms the contact ion-pair structurite shown schematically as

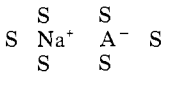

type II structurite

The trigonal character of the field at the anion in this site would be expected to produce C-O stretching vibrations which follow the well-known C_{3v} selection rules. As will be reported elsewhere, the Raman spectrum does not conform to these rules, and similar failures were found for a number of other molecules. The way out of the dilemma was found by proposing that the molecular vibrations in these cases show dual symmetry.[17] According to these ideas, the C-O stretching vibrations of the anion in this site would show C_{3v}/T_d dual symmetry. Each mode will have the symmetry of an irreducible representation (symmetry type) of the C_{3v} group, which characterizes the effective field (geometry) at the anion, as well as the symmetry of an irreducible representation of the T_d group, which characterizes the permutations of the four CO moieties. Then, the F_2 infrared band of the T_d site splits into two infrared bands—an A_1/F_2 band and an E/F_2 band. The A_1/F_2 band arises from the mode of vibration which shows the A_1 symmetry of the C_{3v} group and the F_2 symmetry of the T_d group while the E/F_2 band arises from the two (degenerate) modes which show the E symmetry of C_{3v} and the F_2 symmetry of T_d. The symmetry of the fourth C-O stretching mode is A_1/A_1 and it is inactive in the infrared spectrum through terms in the theory which are first order in the magnitude of the difference between the two kinds of CO moieties.

These spectral expectations correspond to the observations of both type II and type III sites.

The triple ion structurite

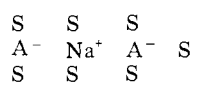

type III structurite

also gives an anion site whose CO stretching spectrum is expected to consist of two bands. Two symmetry cases are possible. The first occurs when there is no coupling between the vibrations of the two anions of the structurite. The CO stretching vibrations (localized at each $Co(CO)_4^-$) shows $C_{3v}{}^I/T_d{}^I$ dual symmetry and the spectral expectations are those discussed above. The second case occurs when there is coupling between the two $Co(CO)_4^-$ moieties. Then, for every mode of a single $Co(CO)_4^-$ there are two modes for the triple ion—one of which involves the mode motion at one anion moving in phase with that at the other anion and the other in which the two motions are out of phase with one another. Only the latter vibration is allowed in the infrared spectrum. Thus, one infrared band is expected in the coupled case for every infrared band expected in the uncoupled case; and one cannot tell from the infrared spectrum alone if the two anions in this structurite are coupled or not. For this reason, the infrared spectrum of the triple ion is treated in terms of the simpler, uncoupled, i.e., localized description of the modes of vibration.

Evidence that the two structurites shown above are responsible for the type II and type III spectra is furnished by conductivity measurements. The equivalent conductance of THF solutions of $NaCo(CO)_4$ was measured at 25 °C over the concentration range 10^{-3}–0.15 M.[18] The value of Λ is about 14 mhos/equiv at the concentration of this study. The conductance data are typical of solutions in which pronounced association of anion and cation take place and imply the presence of both ion pairs and triple ions.[19] Since Λ is falling as the concentration increases at the concentration of this study, the triple ion must be present in the smaller concentration in the THF solution. Thus, the type III site is identified as the triple ion and the type II site as the contact ion pair.

The conductivity data could be qualitatively understood just as well if the triple ion were of the structure

In this case, two of the CO groups of the anion would be associated with Na^+ ions and the other two with solvent molecules. The effective field (geometry) would be C_{2v} and the spectra would be expected to follow the selection rules for the C_{2v}/T_d dual symmetry case. Then, three CO stretching modes would be expected to give rise to strong infrared bands. This type of structure can be eliminated as that of the type III structurite because only two strong infrared bands are observed.

The assignment of the specific infrared bands to the active modes of these sites is given in Table V. Since the band frequencies for a given kind of site are almost independent of the solvent in which it is found (oxetane, 1,2-DME, THF), one can expect that they can be used to identify these sites for $NaCo(CO)_4$ in other similar solvents.

Of these three solutions, only $NaCo(CO)_4$ in THF has been studied before and only over a limited temperature range.[3] Type I and type II sites were identified in that study. The ability of this study to also detect the type III site is the result of the improvements in both the experimental techniques and the analytical methods which have taken place since then. Further, not only does the extended temperature range of this study define the solution structure over its liquid range at and below room temperature, but also the consistency of the results from each temperature is a powerful indication of the correctness of the analysis.

Isotopic Bands. Some comments can be made about the infrared bands from isotopic ions. The $Co(CO)_4^-$ ion with one ^{13}C atom is the only isotopic anion species present in natural abundance at a spectroscopically significant population (4.4 ion percent). It has been shown that when a type I site is occupied by this isotopic ion, the F_2 band is split into an E and an A_1 band.[4] The E band is coincident in frequency with the F_2 band of the normal ion while the A_1 band can be expected about 33 cm^{-1} lower than the F_2 band with an integrated absorbance of 1.5% of that of the main band. Only the type I site (T_d symmetry) is seen in oxetane solutions. The weak side band at 1853 cm^{-1} closely follows the above prescription for the A_1 band from an isotopic ion in this kind of site and is so assigned. The type I site also exists in significant amounts in the 1,2-DME and THF solutions. Hence the A_1 isotopic band is expected in the spectra of these solutions. However, both of these solutions also give rise to an A_1/F_2 band at 1854 cm^{-1} from their type II sites. Further, the THF solution has an A_1/F_2 band from its type III sites at 1846 cm^{-1}. These A_1/F_2 bands would be expected to overlap the A_1 band at 1853 cm^{-1} from the isotopic ion and, with their greater band intensities, it is not expected that the 1853-cm^{-1} isotopic band could be seen as a separate entity. Consequently, no effort was made to introduce it as a separate band in the mathematical analysis of the observed spectral contour. However, a consideration of the computed intensity of the A_1/F_2 bands of the type II and type III sites suggests that part of their intensity arises from the isotopic band. This suggestion is confirmed in the spectrum from the THF solution at 150 K. Here, the increased sharpness of the bands associated with the lower temperature, the increased concentration of the type I sites (>90%), the absence of type III sites, and the low concentration of type II sites, all

acting together, permit the A_1 band from the isotopic ion in type I sites to be clearly seen (see Figure 8) as separate from the weak A_1/F_2 band from the type II sites.

The isotopic ion can be expected to be present also in sites of the type II and type III kinds. An analysis presented in the Barbetta thesis[1] shows that the isotopic bands from these sites are weaker than the A_1 isotopic band discussed above and are expected to be heavily overlapped by stronger bands from the normal ions. Therefore, no separate bands were introduced into the analysis for these isotopic bands, their intensity appearing with that of the bands from the abundant ions.

Influence of the Solvent on Solution Structure. It is possible to understand the differences in the structure of these three solutions in terms of the known properties of the solvent molecules and a simple postulate. It will be assumed that the interaction of the Na^+ ion with a negative center of a neighbor species is the primary interaction which lowers the free energy of these solutions. Then the solution structure is the result of the competition between a solvent molecule and an anion for a position next to the cation. When the interaction of the Na^+ ion with the solvent molecule is much greater than its interaction with the $Co(CO)_4^-$ anion, only type I structurites will exist. As the Na^+ ion–solvent molecule interaction decreases, a point is reached where an occasional solvent molecule next to the Na^+ ion is replaced by a $Co(CO)_4^-$ ion. The type II structurite appears. Further decreases in cation–solvent interaction not only lead to a growth in the amount of the type II structure but eventually to the appearance of the type III structure. In the competition between solvent molecules and anion for position in the near neighbor shell of the Na^+ ion, the donor ability of the electron pair on the oxygen atom of the solvent is of primary importance.

THF is a solvent with good donor ability.[20,21] It is possible to approximate the population of the different structurites in the THF solution from the spectroscopic results reported here and to use the populations to compare the effectiveness of the solvent and the anion in filling a near-neighbor position at the Na^+ ion. This provides a "calibration point" in relating solution structure to solvent properties. The area under the absorption band(s) associated with each kind of solution structure (see Figure 6, right-hand panel) may be taken as approximately proportional to the amount of anion tied up in that structure. In this way, one finds that nearly four-tenths of the (anion containing) solution structurites in THF are type I, almost five-tenths are type II, and somewhat more than one-tenth are type III. These results indicate that the THF molecule is almost as effective as the $Co(CO)_4^-$ anion in obtaining a near-neighbor position at the Na^+ ion as measured by the competing processes

$$S_xNa^+SA^- \rightleftarrows S_xNa^+A^-S$$

Oxetane is a cyclic ether with a four-membered ring. The greater internal strain in this molecule, compared with that in THF with its five-membered ring, increases the donor ability of its oxygen electrons over that of THF. This result is clearly seen in the donor ability measurements for these two ethers.[20] Thus, one expects a greater percent of type I sites in the oxetane solution; and this is indeed found. That the experimental results of this study show *only* type I sites for $NaCo(CO)_4$ in oxetane, compared with the site mix for the THF solution, testifies to the sensitivity of solution structure to the effect of strain in the solvent molecule.

Without the enhancing effect of ring strain, the donor ability of the oxygen electrons of a straight-chain ether such as 1,2-DME is expected to be significantly less than that of THF. And this is indeed found to be the case experimentally.[22] If donor ability were the only effect involved in fixing solution structure, a much smaller fraction of the $NaCo(CO)_4$ ions would be found in type I structurites in 1,2-DME than in THF. However, 1,2-DME can interact with the Na^+ ion in a bidentate manner.

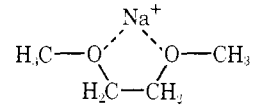

Two, and possibly three, DME molecules can interact with one Na^+ ion in this way. The effect of this chelation is to increase the stability of the type I structurites over that expected for a straight-chain ether capable only of monodentate interaction with the cation. This study finds almost all of the $NaCo(CO)_4$ in type I structurites in 1,2-DME. Thus, the effect of the chelation is to raise the amount of $NaCo(CO)_4$ in type I structurites from the small fraction of the $NaCo(CO)_4$, which is expected on the basis of donor ability alone, to nearly 100%. And one concludes that structure in $NaCo(CO)_4$ solutions is also very sensitive to chelation. These results are in agreement with those of Hogen-Esch and Smid, who also found DME to be a more powerful solvating agent for alkali ions than THF.[23]

This study shows that the effectiveness of these solvents in stabilizing type I sites for $NaCo(CO)_4$ in solution and destabilizing type II and type III sites is

$$\text{oxetane} \sim \text{1,2-DME} > \text{THF}$$

This order can be understood in terms of the variation of the electron donor ability of the solvents and the ability of DME to form a bidentate chelate if one postulates that the competition between solvent molecule and anion for a near-neighbor position at the Na^+ ion is the primary structure-determining event. Studies involving other solvents will add other features to this model.

Some Theoretical Considerations. A quantum treatment of nonaqueous electrolytic solutions has been summarized recently.[13] Despite its approximate character, it permits a useful treatment of some properties of these solutions. Its salient features are outlined here in order to indicate the transitions which give rise to the bands of this study and to make the meaning of the words "structure" and "symmetry" clear for an ion site whose conformation continually changes with time.

The ionic solution can exist in a vast number of quantum states, each of which is associated with a solution energy. Let the position of the ith molecule or ion in the solution be given by a set of coordinates R_i which specify its center of mass and angular orientation. The internal distortion of the ith solvent molecule or molecular ion from its equilibrium configuration (in the solution) is given by a set of coordinates q_i. The electronic states of the solution are treated separately from the rotation, translation, and vibration by the usual adiabatic approximation. The vibratory states of the system are solutions of the equation

$$\{T_q + V(Rq)\}\psi_v(Rq) = W_v(R)\psi_v(Rq) \qquad (4)$$

in which the vibratory states have been separated from those associated with the rotational and translation motion by a second adiabatic approximation. The electronic state dependencies in eq 4 have been suppressed for the sake of a cleaner appearing equation. The kinetic energy operator T_q depends only on (derivatives of) the complete set of distortion coordinates q. V and ψ_v are functions only of the coordinates q but they, like W_v, depend parametrically on the complete set of R coordinates of the solution. The vibrational state of the solution is given by $\psi_v(R)$ and the corresponding energy eigenvalue is $W_v(R)$.

The coupling between the vibration of a molecular ion, e.g., $Co(CO)_4^-$, and the vibration of a neighboring solvent molecule

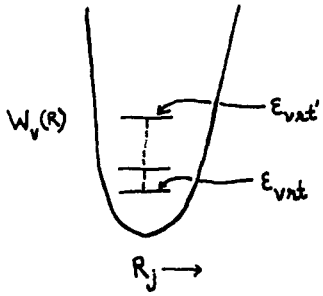

Figure 9. A cross section through the $W_v(R)$ surface in conformation space for conformations of the same solution structure.

is weak because there is no resonance between the modes of the two entities. This coupling is neglected in this treatment. There is no coupling, of course, between the vibration of two ions in the infintely dilute solution. Then $V(Rq)$ can be written in the form

$$V(Rq) = V(R0) + \sum_i V(Rq_i) + V(Rq_s)$$

where $V(R0)$ is the potential energy of the solution in the specific conformation defined by the R and with all molecular entities undistorted. The q_s is the set of distortion coordinates for the solvent molecules and the sum is over all molecular ions in the solution. Under these conditions, eq 4 can be separated to give the vibrational state of each molecular ion ϕ_{v_i} and its energy eigenvalue W_{v_i}. It follows that $W_v(R)$ is given by

$$W_v(R) = V(R0) + \sum_i W_{v_i}(R) + W_{v_s}(R) \qquad (5)$$

where $W_{v_s}(R)$ is the vibrational eigenvalue of the solvent and the other quantities have been defined above.

Equation 4, with eq 5, defines a solution vibratory state ψ_v and energy W_v for a specific conformation of its components. W_v forms a multidimensional surface in R space. When changes in the solution conformation are confined to the vicinity of the ith ion, only W_{v_i} of the ion terms changes significantly, and the change in W_v is made up of it plus the accompanying changes in $V(R0)$ and W_{v_s}. The ith plane through a portion of the W_v surface for such changes is represented schematically in Figure 9.

The energy ϵ of the solution appears as the solution of the equation

$$\{T_R + W_v(R)\}\psi_{rt}(R) = \epsilon_{vrt}\psi_{rt}(R) \qquad (6)$$

Here the dependence of ψ_{rt} on the vibrational and electronic states has been suppressed in the symbolism used. T_R is the kinetic energy operator for the rotation and translation of all the entities of the solution. The vibratory eigenvalue $W_v(R)$ from eq 4 appears as the potential energy in eq 6. The form of $W_v(R)$ will cause the rotational and translational motion of the ions and molecules to be correlated with one another in the rotational-translational states ψ_{rt}. Therefore, rt is a single quantum number. The quantum state of the solution is given by

$$\Psi_{vrt} = \psi_v\psi_{rt}$$

Several energy levels of the solution for the same vth vibrational state but different rotational-translational states are shown in Figure 9. Note that ϵ_{vrt} is the total energy of the solution in the designated state.

This model can be used to describe the quantum states of the solution which are being excited by the infrared radiation to produce the absorption bands of this study. The excitation of a vibratory state of the anion by a photon can be viewed in this model as the excitation of the vibratory state of a single ion. Basic theory of the excitation process shows that this may be accompanied by the simultaneous excitation of a rotational-translational state of the solution. Such a transition from the ground to the first vibrational state in a single anion is described as

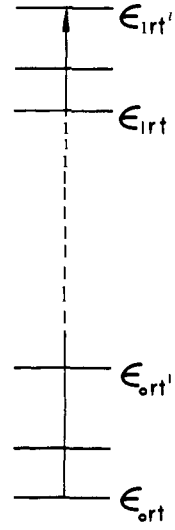

Figure 10. The transition $\Psi_{0rt} \rightarrow \Psi_{1rt'}$.

$$\Psi_{0rt} \rightarrow \Psi_{1rt'}$$

where all the other quantum numbers in v and in rt which do not change have been suppressed. This transition is shown on the energy level diagram of Figure 10. It produces a single line in the absorption band at the wavenumber $\omega = (\epsilon_{1rt'} - \epsilon_{0rt})/hc$. The fundamental band ($0 \rightarrow 1$) consists of the lines from all such transitions, each at its own ω. The transitions

$$\Psi_{0rt} \rightarrow \Psi_{1rt}$$

define the band center and give lines at (or near) the band maximum. The line from the transition

$$\Psi_{0rt'} \rightarrow \Psi_{1rt}$$

occurs on the opposite side of the band center from the first one cited above. The fact that the component bands of this study are essentially symmetrical, as shown so well by the data from the oxetane solutions, implies that the dependency of the rotational-translational contribution to ϵ_{vrt} (as well as that of ω_{rt}) upon v is quite small for the states involved here.

Structure and Symmetry. It is useful to comment on the meaning of the words structure and conformation as used here. How can one define structure in an ionic solution whose components are in constant motion? When all the molecular entities of an ionic solution are undistorted, its potential energy is $V(R0)$. This quantity depends only on the position and orientation of each entity of it relative to some one of them. The set of these relative quantities at an instant in time defines a point in multidimensional conformation space. Each point in conformation space corresponds to a different conformation of the solution. The definition of conformation is completed by specifying that the exchange of identical entities in a conformation does not lead to a new conformation.

$V(R0)$ forms a multidimensional surface when it is plotted against the coordinates of conformation space. Each point on this surface gives the value of $V(R0)$ for a specific conformation. This surface will have a number of pits or depressions corresponding to more stable conformations. All the conformations associated with the same depression are said to be different conformations of the same solution structure. $V(R0)$ makes its primary contribution to the shape and extension of the bands observed in this study.

The center of each band depends upon the energy difference $\epsilon_{1rt} - \epsilon_{0rt}$ corresponding to the excitation of a mode of vibration in an ion of the solution. This difference probes the character of $V(Rq_i)$ through the terms W_{v_i} (v_i being 0 and 1 for the mode of vibration generating the band). Formally, $V(Rq_i)$ depends upon the conformation of the (whole) solution. In reality, however, it depends only on the conformation of the solution in the immediate environs of the vibrating ion. $V(Rq_i)$, for a specific distortion of the ith ion, forms a multidimensional surface when it is plotted against the coordinates of the subdomain of conformation space corresponding to different conformations in the neighborhood of the ion. This surface also has depressions and one can say that each conformation associated with the same depression is a different conformation of the same solution structure at the ion. These local solution structures are the ion sites of this and previous discussions.[2-4] Thus, the positions of the various bands yield information about the different solution structures which exist at the ion being vibrationally excited.

The band center probes the conformation of the ion site at the minimum of a structure depression in the $V(Rq_i)$ surface. A molecular ion will have, in general, a number of modes of vibration. Then, $V(Rq_i)$ at this minimum will be invariant to a set of interchange operations which exchange equivalent internal coordinates.[24] These operations form the elements of a mathematical group which describes the symmetry in the solution structure at the ion site[25] and which gives the selection rules for the vibrations of the ion in this particular ion site. Note that it is the symmetry in the conformation at the $V(Rq_i)$ minimum which is being probed by the band positions and not that a general conformation of the local structure.

One sees that it is possible to speak of symmetry at an ion site even though the conformation there is continually changing. This treatment gives meaning to the phrase "symmetry in the effective force field" which has been used in the previous publications from this laboratory.[3,4]

The fact that the type I ion site shows T_d symmetry indicates that, in the solution conformations of this ion site structure, the local arrangement at one CO group is independent of that at the other three. Thus, it is possible for all four CO groups to look out at the same, low-energy, local arrangement at the same time; and this gives the minimum in this $V(Rq_i)$ depression.

The type II $Co(CO)_4^-$ site has C_{3v} symmetry. This means that the local arrangement at one CO group must be different from those in the other three. Thus, while the three take the same local arrangement in the low-energy conformation, this arrangement is different from that which occurs at the fourth CO group. The same considerations apply to the local arrangements about each $Co(CO)_4^-$ ion in the type III ion site.

Acknowledgment. The authors acknowledge support of this work by the National Science Foundation under Contracts GP 27928 and MPS 74-17322.

References and Notes

(1) Based in part upon Ph.D. Theses of A. Barbetta, Purdue University, 1973, and S. Hegde, Purdue University, 1977.
(2) W. F. Edgell, J. Lyford, IV, A. Barbetta, and C. I. Jose, *J. Am. Chem. Soc.*, **93**, 6403 (1971).
(3) W. F. Edgell and J. Lyford, IV, *J. Am. Chem. Soc.*, **93**, 6407 (1971).
(4) W. F. Edgell and A. Barbetta, *J. Am. Chem. Soc.*, **96**, 415 (1974).
(5) W. F. Edgell and J. Lyford, IV, *Inorg. Chem.*, **9**, 1932 (1970).
(6) A. Barbetta and W. F. Edgell, *Appl. Spectrosc.*, in press.
(7) Air Products and Chemicals, Inc., Allentown, Pa.
(8) W. F. Edgell, "Tracking Error in Spectrometer Operation", unpublished.
(9) "Aldrich Catalog/Handbook of Organic and Biochemicals", Aldrich Chemical Co., 1975-1976.
(10) W. F. Edgell and J. Lyford, IV, *J. Chem. Phys.*, **52**, 4329 (1970).
(11) J. Pitha and R. N. Jones, *Can. J. Chem.*, **44**, 3031 (1966).
(12) J. Pitha and R. N. Jones, *Can. J. Chem.*, **45**, 2347 (1967).
(13) W. F. Edgell in "Practical Spectroscopy", Vol. 1, E. Brame and J. Grasselli, Ed., Marcel Dekker, New York, N.Y., 1976, Chapter 4.
(14) J. Pitha and R. N. Jones, *Natl. Res. Counc. Can. Bull.*, No. 12 (1968).
(15) One of our colleagues has described such a structure as a very soft iceberg.
(16) D. P. Schussler, W. R. Robinson, and W. F. Edgell, *Inorg. Chem.*, **13**, 153 (1974).
(17) W. F. Edgell, *Spectrochim. Acta, Part A*, **31**, 1623 (1975).
(18) W. F. Edgell, M. T. Yang, and N. Koizumi, *J. Am. Chem. Soc.*, **87**, 2563 (1965).
(19) R. Fuoss and F. Accascina, "Electrolytic Conductance", Interscience, New York, N.Y., 1959, Chapters XV-XVIII.
(20) S. Searles, M. Tamres, and E. R. Lippincott, *J. Am. Chem. Soc.*, **75**, 2775 (1953); S. Searles and M. Tamres, *ibid.*, **73**, 3704, (1951).
(21) V. Gutmann, "Coordination Chemistry in Non Aqueous Solutions", Springer-Verlag, West Berlin, 1968.
(22) E. M. Arnett and C. Y. Wu, *J. Am. Chem. Soc.*, **84**, 1684 (1962).
(23) T. E. Hogen-Esch and J. Smid, *J. Am. Chem. Soc.*, **88**, 307 (1966).
(24) Internal coordinates are conveniently chosen to be the changes in the bond lengths and angles of the ion. The normal coordinates of the set q_i are formed by taking appropriate linear combinations of the internal coordinates.
(25) Strictly speaking it is the symmetry in $V(Rq_i)$ that is being described, but any difference between it and the symmetry in the structure need not concern us here.